

## Ultramicroscopy 93 (2002) 179–198

## ultramicroscopy

www.elsevier.com/locate/ultramic

### The S-state model: a work horse for HRTEM

P. Geuens, D. Van Dyck\*

Department of Physics, EMAT, University of Antwerp (RUCA), Groenenborgerlaan 171, 2020 Antwerp, Belgium

Received 15 April 2002; received in revised form 18 July 2002

Dedicated to Peter W. Hawkes on the occasion of his 65th birthday

#### Abstract

The S-state model describes the dynamical scattering of electrons in a specimen foil, consisting of atom columns parallel to the beam direction, such as a crystal or a particular crystal defect. In this model the electrons are considered to be trapped in the electrostatic potential of an atom column, in which it scatters dynamically. This picture allows physical insight, and it explains why a one-to-one correspondence is maintained between the exit wave and the projected structure, even in case of strong dynamical scattering. Furthermore the model can be parameterised in a simple closed analytical form. Apart from the computational advantages, the S-state model proves to be very useful to deduce the projected structure directly from the exit wave, so as to "invert" the dynamical scattering. In this paper the validity of the S-state model, is evaluated in much depth by a proper quantum mechanical treatment. The analytical parameterisation of the 1S eigenfunction and eigenenergy is discussed. It is shown that the method, even in case of small tilts, is valid for most thicknesses, currently used in HRTEM studies. Even for closely spaced atom columns, such as the dumbbells in Si [1 1 0], Sn [1 1 0] and GaN [1 1 0], the positions of the atom columns can be deduced with an accuracy of a few pm.

© 2002 Elsevier Science B.V. All rights reserved.

PACS: 61.14.Dc; 61.16.Bg

Keywords: High-resolution transmission electron microscopy (HRTEM); Electron diffraction and elastic scattering theory; Image simulation

#### 1. Introduction

Due to the imaging in an electron microscope and multiple scattering of electrons in the specimen foil, a high-resolution transmission electron microscope (HRTEM) image is hard to interpret in terms of its structure, not to mention determi-

E-mail address: dvd@ruca.ua.ac.be (D. Van Dyck).

nation of atom column positions, with high precision. To determine the structure from an electron micrograph the imaging and scattering must, in a sense be inverted.

In the past, methods were proposed to eliminate the blurring effect of the microscope, by reconstruction of the exit wave [1-5] or by correction for spherical aberration ( $C_s$ ) [6]. These reconstructed electron waves [7-9] and  $C_s$ -corrected images [10,11], are much sharper than conventional HRTEM images. Nevertheless they are not yet

<sup>\*</sup>Corresponding author. Tel.: +32-3-2180258; fax: +32-3-21803318.

interpretable in terms of positions and mass of the atom columns. Therefore the dynamical scattering must be inverted, so as to obtain a starting structure which can be used as a "seed" for further quantitative structure refinement.

Plane wave based methods, like the multislice and Bloch wave formalism, are not useful for this purpose, since they do not explain on an intuitive basis why, even in case of highly dynamical scattering, the HRTEM exit wave is still locally related to the projected structure. The classical picture of electrons crossing the crystal as plane like waves in the directions of the Bragg-beams, which stems from X-ray diffraction, is in fact misleading. The physical reason for this local dynamical diffraction is the channelling of the electrons along the atom columns parallel to the beam direction. Due to the positive electrostatic potential of the atoms, an atom column acts as a guide or channel for an electron. In an atom column the electron can scatter dynamically without leaving it. The channelling theory [12-18] describes this effect and thus provides such physical insight. The fundamental principle is actually very closely related to a set of converging lenses in a row, illuminated by a plane wave like light wave. The light will be focused to a point at a certain distance, depending on the strength of the lenses and the repeat distance, and will be a plane wave again at twice this distance. This effect will be repeated periodically. The principle of the channelling theory is based on the expansion of the electron wavefunction in eigenfunctions of the averaged atom column potential along the column. It turns out that this basis is so effective that the scattering of the electron can be described fairly well using only one bound eigenfunction, the 1S eigenfunction. The electron wavefunction can be represented as a simple and even analytic expression, if the 1S eigenfunction is parameterised, which allows fast calculation. At the other hand, it explains why the motion of the electron along the atom column is nearly periodical.

Because of its simplicity, the method has the potential to become a real work horse for HRTEM. It permits interpretation of the reconstructed electron wavefunction directly in terms of the projected structure, yielding an approximate

structure model that can then further be used as a starter for quantitative refinement. Furthermore it is valid even for crystal defects (dislocations, translation interfaces, etc.) as long as the atoms are aligned in columns in a direction close to the beam direction.

The concept of channelling is not new. Lindhard did the first experiments based on classical particle scattering by studying the blocking effect on natural alpha particle emission from <sup>222</sup>Rn atoms implanted in W [19]. The quantum mechanical treatment of the channelling of energetic electron beams was developed by Tamura et al. [20] and Fujimoto [21]. The theory of diffraction channelling was given in a form applicable to experiments with fast electrons and positrons by Howie [12]. The analogy with atomic wavefunctions has been developed extensively by Buxton, Steeds and co-workers for the interpretation of CBED patterns [22].

This paper is organised as follows. In Section 2 the basic assumptions are posed together with a summary of the main results of the channelling theory. The thickness range for which the S-state model, for isolated atom columns, is valid is estimated. An expression for the electron wavefunction is proposed in closed analytic form in Section 3. The physical evidence of the model and a theoretical indication for the parameterisation of the 1S eigenenergy, are discussed as well. In order to study the effect of neighbouring atom columns on the S-state model, the explicit case of atom columns in diamond type of structures, like Si and Sn, and GaN, all in [110] orientation, are considered, in Section 4. The results can be generalised in a straightforward manner to a columnar structure in zone-axis orientation. It will be shown that to a good approximation the wavefunction of a columnar structure can be described by the superposition of the wavefunctions of the respectively constituting atom columns, for the thickness range commonly used in HRTEM and that atom column positions can be determined with an accuracy up to a few pm. In the last section, tilt is included in the model.

For the presented calculations a Doyle and Turner [23] parameterisation was used for the electron scattering factors to calculate the twodimensional mean atom column potentials. The kinetic energy of the incident electrons was assumed to be 300 keV and the Debye–Waller factor 0.006 nm<sup>2</sup>.

# 2. Electron channelling theory for an isolated atom column

The central assumption, on which the approximations of the channelling theory are based, is that the energy of the incident electrons is several orders of magnitude larger than the potential energy of the foil. In this case it is convenient to consider the exit wave as a modulated plane wave, with  $\Psi(\mathbf{R},z)$  the modulation function. **R** is a twodimensional vector parallel to the foil surface and z is a one-dimensional vector perpendicular to **R** with opposite sign as the beam direction. The first approximation is the "forward scattering approximation" or "paraxial approximation", which assumes that the second order derivative of the modulation function is small and can be neglected, since the motion of the high-energy electrons is predominant in the forward z-direction. The second approximation states that, the potential energy, felt by an electron in the foil, can be assumed to be proportional to the averaged twodimensional potential  $U(\mathbf{R})$  along the z-direction, which is equivalent to the neglect of the higher order Laue zones. In this sense, the electron channelling is a high-energy approximation, suitable for situations in which the incident beam direction is parallel or close to parallel to a main zone-axis. The latter will be discussed in more detail later on in this paper. Now a plane wave illumination along a main zone-axis is assumed. The main result of the channelling theory, for details we refer to Refs. [13-17], is that the wavefunction of an atom column is given by

$$\Psi(\mathbf{R}, z) = 1 + \sum_{nm} 2c_{nm} \sin\left(\pi \frac{-E_{nm}}{E_0} \frac{k_z}{2} z\right) \psi_{nm}(\mathbf{R})$$

$$\times \exp\left\{-i\pi \left(\frac{E_{nm}}{E_0} \frac{k_z}{2} z - \frac{1}{2}\right)\right\},\tag{1}$$

where  $c_{nm}$  are the excitation coefficients,  $\psi_{nm}(\mathbf{R})$  the eigenfunctions of the Hamiltonian with eigenenergies  $E_{nm}$ ,  $E_0$  the kinetic energy of the incident

electron,  $k_z = 1/\lambda$  the z-component of the wavevector of the incident plane wave, with  $\lambda$  the relativistic electron wavelength and z the specimen foil thickness.  $\psi_{nm}(\mathbf{R})$  and  $E_{nm}$  are solutions of the eigenvalue problem

$$H\psi_{nm}(\mathbf{R}) = E_{nm}\psi_{nm}(\mathbf{R})$$
 with 
$$H = -\frac{\hbar^2}{2\mu}\Delta_{\mathbf{R}} - eU(\mathbf{R}), \tag{2}$$

with  $\Delta_{\mathbf{R}}$  the two-dimensional Laplacian operator acting in the plane, parallel to the specimen surface and perpendicular to z, and  $\mu$  the relativistic electron mass.

n and m are respectively the main- and angular-quantum number. The quantum numbers classify the eigenfunctions in a similar way as the eigenfunctions of the two-dimensional quantum harmonic oscillator. The same restrictions to m, as for the two-dimensional harmonic oscillator, are valid, i.e. m = -n, -n + 2, ..., n - 2, n with n = 0, 1, 2, ... an integer number. The wavefunction is now described in terms of the eigenfunctions  $\psi_{nm}(\mathbf{R})$  and eigenenergies  $E_{nm}$  of the two-dimensional Hamiltonian. Methods to calculate the bound eigenfunction of an isolated atom column will be discussed in Appendix A.

It was shown in Ref. [15] that the excitation coefficients  $c_{nm\neq 0} = \int \psi_{nm\neq 0}^*(\mathbf{R}) d\mathbf{R}$  are zero, since the integral over the space of Eq. (A.2) is zero. The wavefunction of an isolated atom column, is thus rotationally symmetric  $\Psi(\mathbf{R}, z) = \Psi(\rho, z)$ , with  $|\mathbf{R}| = \rho$ . For most atom columns, only one eigenfunction is bound,  $\psi_{00}(\rho)$ . In previous papers about channelling, this eigenfunction was called the 1S eigenfunction, in similarity with the hydrogen atom. Note that this spectroscopic notation stems from the labeling of the eigenfunctions of a three-dimensional one-electron atom. Here the problem is two-dimensional. Nevertheless this nomenclature will be used throughout this paper to avoid confusion with previous papers. The subscript of the 1S eigenfunction will be kept "00".

For heavier atom columns (e.g. Sr [1 0 0] and Au [1 0 0]) also  $\psi_{20}(\rho)$  is bound, albeit only weak compared to  $\psi_{00}(\rho)$ . Since  $|E_{20}|$  is much smaller than  $|E_{00}|$  the relative importance of  $\psi_{20}(\rho)$  is much

smaller and is building up much slower as function of thickness compared to  $\psi_{00}(\rho)$ . This is clear from Fig. 1 where

$$\left| c_{00} \sin \left( \pi \frac{-E_{00}}{E_0} \frac{k_z}{2} z \right) \right|$$

and

$$\left| c_{20} \sin \left( \pi \frac{-E_{20}}{E_0} \frac{k_z}{2} z \right) \right|$$

are plotted for various atom column types as function of thickness. From this graph it can be concluded that restricting the expansion to  $\psi_{00}(\rho)$  is a valid approximation, for an isolated atom column, up to a thickness of about 80% of  $D_{00} = -(2/k_z)(E_0/E_{00})$ , the periodical thickness. This can be taken as a rule of thumb for the validity of the S-state model for an isolated atom column. The thickness of the specimen foil used in high-resolution electron microscopy is mostly in that range. The wavefunction can thus to good approximation be written as

$$\Psi(\rho, z) \simeq 1 + 2c_{00} \sin\left(\pi \frac{-E_{00}}{E_0} \frac{k_z}{2} z\right) \psi_{00}(\rho) \times \exp\left\{-i\pi \left(\frac{E_{00}}{E_0} \frac{k_z}{2} z - \frac{1}{2}\right)\right\}.$$
(3)

This expression is known as the S-state model. Note that the S-state model is valid for incident

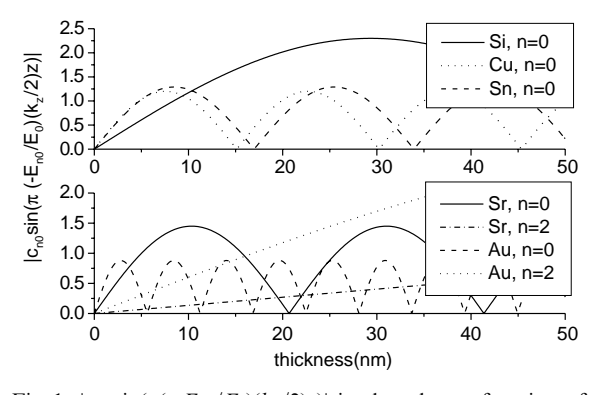


Fig. 1.  $|c_{n0} \sin(\pi(-E_{n0}/E_0)(k_z/2)z)|$  is plotted as a function of specimen foil thickness, for all n, for which  $E_{n0} < 0$ . The repeat distance d in the atom column is respectively for Si, Cu, Sr, Sn and Au: 0.5431, 0.3615, 0.608, 0.6489 and 0.40786 nm. Note that the  $|c_{n0} \sin(\pi(-E_{n0}/E_0)(k_z/2)z)|$  oscillates faster for heavier atom columns.

electrons with a kinetic energy in the intermediate range, i.e. 100–300 keV, and is not valid for high kinetic energies (e.g. 1 MeV), for which more rotationally symmetric eigenfunctions are bound.

In the forgoing, no absorption was taken into account, although the high-energetic incident electrons have enough energy to excite atoms and phonons in the specimen foil. The electron is then scattered inelastically. The total amount of elastically scattered electrons is therefore reduced. This effect of absorption can be modelled by introducing an imaginary two-dimensional mean atom column potential [24], which is proportional to the original one,  $U_a(\mathbf{R}) = (1+\mathrm{i}\gamma)U(\mathbf{R})$  [25]. This will affect the eigenenergy, which is now complex, as well as the periodical thickness  $D_{00}$  and will introduce an exponential damping.

# 3. Parameterisation of the 1S eigenfunction and eigenenergy of an isolated atom column

Empirically it was shown [15,26,27] that  $E_{00}$  can be approximately parameterised in function of the atomic number Z, the repeat distance in the atom column d and the Debye–Waller factor B as [27]

$$\frac{1}{|E_{00}|} = \alpha \left(\frac{d^2}{Z} + \beta B\right). \tag{4}$$

In this section, we like to give a theoretical indication for this expression.

From calculations and prior work [16,26,28] it can be concluded that, the 1S eigenfunctions have a shape which is in between an exponential function and a Gaussian.

First, we assume that B = 0. In this case, all atoms are perfectly aligned in the atom column. The atom column potential is then sharply peaked at the atom column core, as is the 1S eigenfunction. Therefore it can be assumed that the 1S eigenfunction is well described by a two-dimensional normalised exponential function of the form

$$\psi_{00}(\rho) = \sqrt{\frac{|E_{00}^{B=0}|}{2\pi}} \frac{1}{b} \exp\left(-\frac{1}{2} \left(\frac{\sqrt{|E_{00}^{B=0}|\rho}}{b}\right)\right). \quad (5)$$

By substitution of Eq. (5) in Eq. (2) it can be shown mathematically, that the atom column

potential is inversely proportional to  $\rho$  and since it is averaged along the beam direction it is inversely proportional to d

$$U(\rho, B = 0) = \frac{C}{d} \frac{1}{\rho},\tag{6}$$

with C a proportionality factor. Such coulombic string potentials were used in the past to describe rosette-motion channelling [29,30]. The eigenenergy can then be calculated as

$$E_{00}^{B=0} = \frac{\int_0^\infty \psi_{00}^*(\rho) H \psi_{00}(\rho) \rho d\rho}{\int_0^\infty |\psi_{00}(\rho)|^2 \rho d\rho}$$
(7a)

After substitution of Eq. (5) in Eq. (7a), Eq. (7a) is equal to

$$E_{00}^{B=0} = \frac{C}{d} \frac{\int_0^\infty \exp\left(-\left(\frac{\sqrt{|E_{00}^{B=0}|}\rho}{b}\right)\right) d\rho}{\int_0^\infty \exp\left(-\left(\frac{\sqrt{|E_{00}^{B=0}|}\rho}{b}\right)\right) \rho d\rho}$$
$$= \frac{C}{d} \frac{\sqrt{|E_{00}^{B=0}|}}{b}, \tag{7b}$$

or

$$\frac{1}{|E_{00}^{B=0}|} = \frac{b^2}{C^2} d^2,\tag{8}$$

with H the Hamiltonian. From comparison of Eqs. (8) and (4) it can be concluded that

$$\frac{b^2}{C^2} \simeq \frac{\alpha}{Z'},\tag{9}$$

with  $\alpha$  independent of Z, d and B, i.e. independent of the type of atom column.

Secondly, we assume that  $B \neq 0$ . In this case the atoms are no longer perfectly aligned in the atom column due to thermal motion. As a result,  $U(\rho, B \neq 0)$  is broadened and flattened. If the atom column potential is broadened the 1S eigenfunction will be broader as well. Let us therefore assume that the 1S eigenfunction is well described as a Gaussian. It can be proven mathematically, by substitution into Eq. (2), that the atom column potential is then quadratic, which is equal to a Gaussian up to second order in  $\rho$ 

$$U(\rho, B \neq 0) \propto \alpha \beta |E_{00}^{B \neq 0}| \exp(-4\pi^2 \alpha \beta |E_{00}^{B \neq 0}|\rho^2).$$
 (10)

The broadening of  $U(\rho, B \neq 0)$  due to thermal motion can be described by a convolution of  $U(\rho, B = 0)$  and a Gaussian damping function proportional to  $(1/B) \exp(-4\pi^2 \rho^2/B)$ . Assume now for simplicity that also  $U(\rho, B = 0)$  is Gaussian, in analogy with the usual parameterisation of the electron scattering factors [23].

$$U(\rho, B = 0) \propto \alpha \beta |E_{00}^{B=0}| \exp(-4\pi^2 \alpha \beta |E_{00}^{B=0}|\rho^2).$$
 (11)

For 
$$B \neq 0$$
,  $U(\rho, B \neq 0)$  is then
$$U(\rho, B \neq 0) \propto \frac{1}{1/\alpha\beta |E_{00}^{B=0}| + B}$$

$$\times \exp\left(-4\pi^2 \frac{\rho^2}{1/\alpha\beta |E_{00}^{B=0}| + B}\right). \quad (12)$$

From Eqs. (12) and (10), it follows that

$$\frac{1}{|E_{00}^{B\neq0}|} = \alpha \left(\frac{d^2}{Z} + \beta B\right). \tag{13}$$

A similar expression is obtained as in Eq. (4). Eq. (13) is not an exact expression for  $E_{00}$ , but an approximate one and can be used as a rule of thumb.

Note that the inverse of Eq. (13) (B = 0) looks very similar to  $\alpha_a$ , defined in Ref. [31], as a parameter which describes the strength of interaction of electrons and the specimen foil. If  $\alpha_a$  is larger than unity, many wave diffraction effects become important. In this case the classical model becomes applicable.

If the Debye-Waller factor is large, a quadratic normalised two-dimensional Gaussian will be preferable and sufficient to a good approximation

$$\psi_{00}(\rho) = \sqrt{\frac{|E_{00}|}{\pi}} \frac{1}{b} \exp\left(-\frac{1}{2} \left(\frac{\sqrt{|E_{00}|}\rho}{b}\right)^2\right). \tag{14}$$

If the Debye–Waller factor is small, a quadratic normalised two-dimensional exponential function is preferable and sufficient to a good approximation

$$\psi_{00}(\rho) = \sqrt{\frac{|E_{00}|}{2\pi}} \frac{1}{b} \exp\left(-\frac{1}{2} \left(\frac{\sqrt{|E_{00}|}\rho}{b}\right)\right). \tag{15}$$

 $<sup>^{1}</sup>$  In Ref. [15] a different exponent of d is proposed, but this is within the error of the approximation.

By substitution of Eq. (14) or Eq. (15) in Eq. (3) the wavefunction is expressed in a closed analytical form, which allows fast computation and taking analytical derivatives. Note that a Gaussian has the main advantage that also its Fourier transform has a simple analytic expression. The analytic S-state model is in this case also applicable in Fourier space.

In Appendix B a fast calculation method, to estimate the approximate 1S eigenfunction and eigenenergy, is presented assuming that the 1S eigenfunction has a Gaussian- or exponential shape.

# 4. Electron channelling theory for non-isolated atom columns

#### 4.1. Introduction

Up to now the wavefunction of an isolated atom column was considered. In this section we will show that the wavefunction of an assembly of parallel atom columns, can to a good approximation be described by the superposition of the wavefunctions of the respectively constituting atom columns, at least if the atom columns are not too closely spaced. For simplicity, we will consider a two-atom column system. The results can be generalised for general assemblies of atom columns. In this case the Hamiltonian is equal to

$$H = -\frac{\hbar^2}{2\mu} \Delta_{\mathbf{R}} - eU^a(\mathbf{R} - \mathbf{R}_a) - eU^b(\mathbf{R} - \mathbf{R}_b), \quad (16)$$

with  $\mathbf{R}_a$  the position of the first atom column and  $\mathbf{R}_b$  the position of the second one. Similarly as for an isolated atom column the wavefunction can be expanded in eigenfunctions of the Hamiltonian,

$$\Psi(\mathbf{R}, z) = 1 + \sum_{p} 2c_{p} \sin\left(\pi \frac{-E_{p}}{E_{0}} \frac{k_{z}}{2} z\right) \psi_{p}(\mathbf{R})$$

$$\times \exp\left\{-i\pi \left(\frac{E_{p}}{E_{0}} \frac{k_{z}}{2} z - \frac{1}{2}\right)\right\},\tag{17}$$

 $\psi_p(\mathbf{R})$  are solutions of the second-order, linear, partial differential equation  $H\psi_p(\mathbf{R}) = E_p\psi_p(\mathbf{R})$ , where p labels the eigenfunctions. Exact solutions of this equation are, in contrast with the isolated atom column case, not easily accessible. Approx-

imate solutions can be obtained by expansion of the unknown eigenfunctions in a complete set of basis functions. A complete set usually contains an infinite number of elements. In this case, little is accomplished, unless it is a basis set with the desirable property that only a small number of functions contribute significantly to the sum. Two familiar sets for a two-atom column system are  $\{\psi_{nm}^{a}(\mathbf{R})\}\$ , the set of isolated atom column eigenfunctions localised at atom column a and  $\{\psi_{nm}^b(\mathbf{R})\}\$ , the set of isolated atom column eigenfunctions localised at atom column b. Each set is complete and consists of orthonormal functions. Although, in principle one can expand  $\psi_p(\mathbf{R})$  only in terms of  $\{\psi_{nm}^a(\mathbf{R})\}\$ , one needs a very large number of eigenfunctions to describe the behaviour at atom column b. The solution is, to use the collection of all eigenfunctions on a and b as a basis set. In most cases, only a few eigenfunctions are needed. However this set has one disadvantage, that the eigenfunctions of different atom columns are not orthonormal to each other. Symmetry arguments, together with qualitative insight, can be used to decide which basis functions to keep. Note that the expansion of  $\psi_p(\mathbf{R})$  in functions of  $\{\psi_{nm}^a(\mathbf{R})\}$  and  $\{\psi_{nm}^b(\mathbf{R})\}$ allows one to learn about the relation between eigenfunctions of a columnar structure and eigenfunctions of an isolated atom column.

#### 4.2. Symmetry arguments

Columnar structures and crystals are characterised by certain symmetry operations which permit classification of the  $\psi_n(\mathbf{R})$  eigenfunctions. Some symmetry operations leave the Hamiltonian of the system unchanged. In two dimensions the possible symmetry operations are limited to the 10 two-dimensional crystallographic point groups. Nevertheless, for a two-atom column system the possible symmetry operations are limited. The point group is  $2m_h m_v$  for an identical two-atom column system and  $m_h$  for a non-identical twoatom column system, with 2 a rotation over  $\pi$ radians,  $m_h$  a horizontal mirror axis and  $m_v$  a vertical mirror axis. In both cases, the Hamiltonian commutes with  $m_h$ . The eigenfunctions are classified according to their behaviour when acted on by this operation

$$m_{\rm h}\psi_{\sigma}(\mathbf{R}) = \psi_{\sigma}(\mathbf{R})$$
 ( $\sigma$  eigenfunction),  
 $m_{\rm h}\psi_{\pi}(\mathbf{R}) = -\psi_{\pi}(\mathbf{R})$  ( $\pi$  eigenfunction). (18)

The eigenfunctions have a second label according to their rank in energy (1, 2, 3, ...). In the identical atom column case the Hamiltonian is also invariant under inversion  $\mathcal{I} = m_h m_v = 2$ , which demands a third classification

$$\mathcal{I}\psi_{\rm g}(\mathbf{R})=\psi_{\rm g}(\mathbf{R})$$
 (gerade eigenfunction), 
$$\mathcal{I}\psi_{\rm u}(\mathbf{R})=-\psi_{\rm u}(\mathbf{R})$$
 (ungerade eigenfunction). (19)

Summarising, there are four possible symmetries for eigenfunctions of the identical two-atom

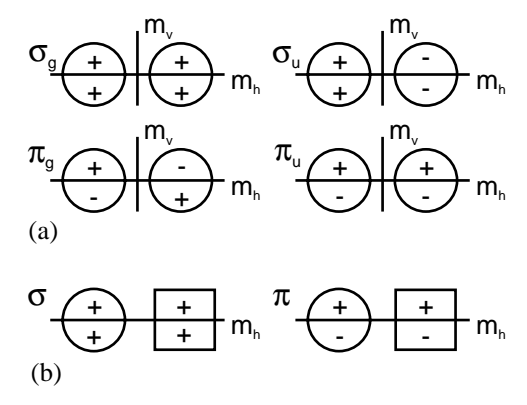


Fig. 2. Possible symmetries of the eigenfunctions of an identical (a) and a non-identical (b) two-atom column system. The relative sign of the eigenfunction (+ or -) is shown in each case.

column system  $\sigma_g$ ,  $\sigma_u$ ,  $\pi_g$ ,  $\pi_u$  and two possible symmetries for eigenfunctions of the non-identical two-atom column system  $\sigma$ ,  $\pi$ . These symmetries are illustrated in Fig. 2, where the signs in each quadrant denote the relative sign of the eigenfunction.

It can easily be understood that, in the expansion of an eigenfunction of the two-atom column system, only these isolated atom column eigenfunctions appear that have the same symmetry. Note that in case of plane wave illumination along a main zone-axis, the " $\pi$  eigenfunctions" and "ungerade eigenfunctions" are not excited, which can be concluded from symmetry arguments.

Each eigenfunction  $\psi_n(\mathbf{R})$  has a certain symmetry classified above and an associated eigenenergy  $E_p$ , that is function of the inter atom column distance D. Hence it would be useful to represent, on a diagram the eigenenergy of each eigenfunction as function of D together with its symmetry. Such a schematic sketch is called a correlation diagram. Fig. 3a shows the correlation diagram for two identical atom columns. The extremes, of the graph, show the eigenfunctions for infinitely spaced atom columns (right) and for fully coincident atom columns (left). The eigenfunctions with the same symmetry are connected; the lowest (D=0) to the lowest  $(D=\infty)$ , the next lowest (D=0) to the next lowest  $(D=\infty)$ , and so on. Fig. 3b shows the correlation diagram for the nonidentical atom column case. Similarly to the identical atom column case the eigenfunctions are classified according to their symmetry and are

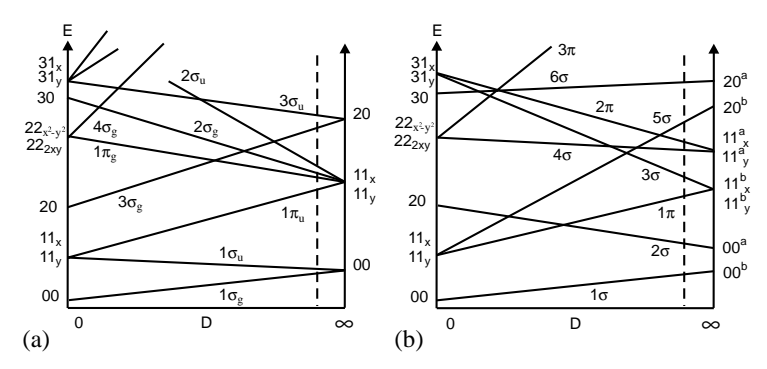


Fig. 3. (a) Correlation diagram of a two-dimensional identical two-atom column system, showing the lowest 11 eigenfunctions. (b) Correlation diagram of a two-dimensional non-identical two-atom column system, showing the lowest nine eigenfunctions. The dotted line marks the realistic inter atom column distance *D* region for columnar structures in a main zone-axis orientation.

connected. The eigenfunctions of the atom columns in the non-identical atom column case are non-degenerated, here is assumed that the energy levels of atom column a are higher than the energy levels of atom column b. This scheme is discussed in more detail for three-dimensional molecules in Ref. [32], which is very similar.

Sketches of the eigenfunctions of an identical and non-identical two-atom column system can be generated using the correlation diagrams in Fig. 3a and Fig. 3b, respectively. For example, in case of an identical two-atom column system, the  $1\sigma_g$  eigenfunction emerges from two isolated 1S eigenfunctions with the same eigenenergy and must change continuously in a 1S isolated atom column eigenfunction, as D decreases from  $\infty$ . In the meanwhile the  $\sigma$  symmetry must be preserved for all D. A sketch of the  $1\sigma_g$  eigenfunction, in the extreme limits and for an intermediate D, is shown in Fig. 4 as well as some other eigenfunctions. Fig. 5 shows some sketches of eigenfunctions in case of a non-identical two-atom column system.

At the other hand, the correlation diagrams can be used to decide which isolated atom column eigenfunctions contribute most to a particular two-atom column system eigenfunction  $\psi_p(\mathbf{R})$ . In the range between D=0 and  $\infty$  also other

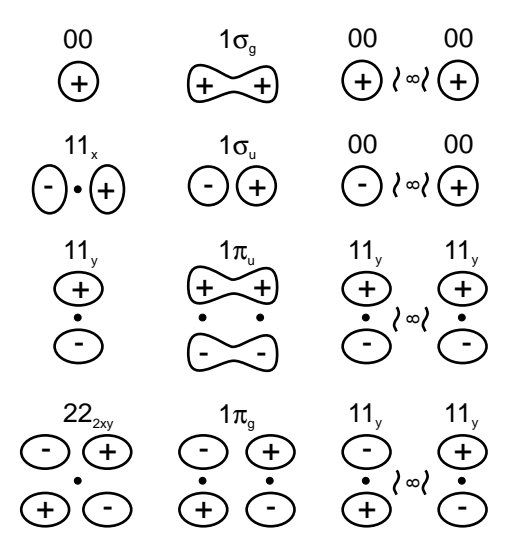


Fig. 4. Sketches of the eigenfunctions of an identical two-atom column system, in the extreme limits (D=0, at the left) and ( $D=\infty$ , at the right) and for intermediate inter atom column distances D. The points denote the atom column positions.

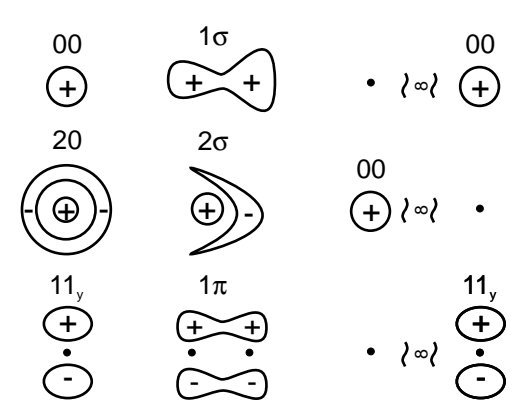


Fig. 5. Sketches of the eigenfunctions of an non-identical two-atom column system, in the extreme limits (D=0, at the left) and ( $D=\infty$ , at the right) and for intermediate inter atom column distances D. The points denote the atom column positions.

isolated atom column eigenfunctions besides  $\psi_{00}$ can contribute to  $1\sigma_g$  as long as the symmetry requirements are fulfilled. In the next sections the relevance of the various two-atom column system eigenfunctions and the various isolated atom column eigenfunctions in the expansion are studied. Note that in HRTEM in a main zoneaxis orientation the inter atom column distances are close to the  $D = \infty$  case, which implies that the atom columns to a very good approximation can be considered as isolated and the mutual overlap can be considered as a perturbation. This will be discussed later on. Note that we exclude here atom columns which have a zig-zag arrangement, which in a first approximation can be regarded as a single atom column with a large Debye-Waller factor.

#### 4.3. Identical two-atom column system

In the case of an identical two-atom column system,  $\{E^a_{nm}\}$  and  $\{E^b_{nm}\}$  are equal, which means that they are degenerated. As stated above, only the  $\sigma_g$  eigenfunctions are excited, in case of plane wave illumination along a main zone-axis, which could be concluded from symmetry arguments. In this paragraph only the  $\psi^a_{00}(\mathbf{R})$  and  $\psi^b_{00}(\mathbf{R})$  eigenfunctions will be taken into account in the expansion of  $\psi_{1\sigma_g}(\mathbf{R})$ . In principle,  $\psi^a_{11_x}(\mathbf{R})$ ,  $\psi^b_{11_x}(\mathbf{R})$ ,  $\psi^a_{20}(\mathbf{R})$  and  $\psi^b_{20}(\mathbf{R})$  could be included in the expansion since they have the appropriate symmetry,

although it is expected that these eigenfunctions will contribute much less than  $\psi_{00}^a(\mathbf{R})$  and  $\psi_{00}^b(\mathbf{R})$ . The degree to which  $\psi_{11_x}^a(\mathbf{R})$ ,  $\psi_{11_x}^b(\mathbf{R})$  will contribute, depends on the overlap of these eigenfunctions and thus on the separation between the atom columns. It is one of the aims of this paper to show that expansion of  $\psi_{1\sigma_g}(\mathbf{R})$  only in  $\psi_{00}^a(\mathbf{R})$  and  $\psi_{00}^b(\mathbf{R})$  is rather sufficient and that to a good approximation the expansion of  $\Psi(\mathbf{R},z)$  can be limited by only taking  $\psi_{1\sigma_g}(\mathbf{R})$  into account.  $\psi_{1\sigma_g}(\mathbf{R})$  can be written as

$$\psi_{1\sigma_{g}}(\mathbf{R}) \simeq a_{00}^{1\sigma_{g}} \psi_{00}^{a}(\mathbf{R} - \mathbf{R}_{a}) + b_{00}^{1\sigma_{g}} \psi_{00}^{b}(\mathbf{R} - \mathbf{R}_{b}), \quad (20)$$

where  $a_{00}^{1\sigma_g}$  is equal to  $b_{00}^{1\sigma_g}$  since  $\psi_{1\sigma_g}(\mathbf{R})$  is invariant under inversion. Substitution of Eq. (20) in Eq. (17) becomes

$$\Psi(\mathbf{R}, z) \simeq 1 + 2c_{1\sigma_{g}}c_{00}^{1\sigma_{g}}\sin\left(\pi \frac{-E_{1\sigma_{g}}}{E_{0}} \frac{k_{z}}{2}z\right) 
\times (\psi_{00}^{a}(\mathbf{R} - \mathbf{R}_{a}) + \psi_{00}^{b}(\mathbf{R} - \mathbf{R}_{b})) 
\times \exp\left\{-i\pi\left(\frac{E_{1\sigma_{g}}}{E_{0}} \frac{k_{z}}{2}z - \frac{1}{2}\right)\right\},$$
(21)

where  $a_{00}^{1\sigma_{\rm g}}$  and  $b_{00}^{1\sigma_{\rm g}}$  are set to  $c_{00}^{1\sigma_{\rm g}}$ . The next bound eigenfunction of the two-atom column system, which is neglected in the equation above is  $\psi_{2\sigma_{\rm g}}(\mathbf{R})$ , can mainly be described as a linear combination of  $\psi_{11_x}^a(\mathbf{R})$  and  $\psi_{11_x}^b(\mathbf{R})$ . This could be concluded from the correlation diagram in Fig. 3a. This eigenfunction will contribute much less than  $\psi_{1\sigma_{\rm g}}(\mathbf{R})$  and was therefore neglected.

#### 4.4. Non-identical two-atom column system

In the case of a non-identical two-atom column system, it may be supposed that  $E^a_{00} > E^b_{00}$ , since,  $\psi^a_{00}(\mathbf{R})$  and  $\psi^b_{00}(\mathbf{R})$  are non-degenerate, in contrast with the identical two-atom column system. Also here, the expansion of  $\psi_{1\sigma}(\mathbf{R})$  and  $\psi_{2\sigma}(\mathbf{R})$  are limited to  $\psi^a_{00}(\mathbf{R})$  and  $\psi^b_{00}(\mathbf{R})$  and the expansion of  $\Psi(\mathbf{R}, z)$  is limited to the two most bound eigenfunctions  $\psi_{1\sigma}(\mathbf{R})$  and  $\psi_{2\sigma}(\mathbf{R})$ , which can be written as

$$\psi_{1\sigma}(\mathbf{R}) \simeq a_{00}^{1\sigma} \psi_{00}^{a}(\mathbf{R} - \mathbf{R}_{a}) + b_{00}^{1\sigma} \psi_{00}^{b}(\mathbf{R} - \mathbf{R}_{b}),$$
 (22)

$$\psi_{2\sigma}(\mathbf{R}) \simeq a_{00}^{2\sigma} \psi_{00}^a(\mathbf{R} - \mathbf{R}_a) + b_{00}^{2\sigma} \psi_{00}^b(\mathbf{R} - \mathbf{R}_b).$$
 (23)

Substitution of Eqs. (22) and (23) into Eq. (17) results in

$$\Psi(\mathbf{R}, z) \simeq 1 - (c_{1\sigma}a_{00}^{1\sigma} + c_{2\sigma}a_{00}^{2\sigma})\psi_{00}^{a}(\mathbf{R} - \mathbf{R}_{a}) 
- (c_{1\sigma}b_{00}^{1\sigma} + c_{2\sigma}b_{00}^{2\sigma})\psi_{00}^{b}(\mathbf{R} - \mathbf{R}_{b}) 
+ \left(c_{1\sigma}a_{00}^{1\sigma}\exp\left\{-i\pi\frac{E_{1\sigma} - E_{2\sigma}}{E_{0}}k_{z}z\right\}\right) 
+ c_{2\sigma}a_{00}^{2\sigma}\psi_{00}^{a}(\mathbf{R} - \mathbf{R}_{a})\exp\left\{-i\pi\frac{E_{2\sigma}}{E_{0}}k_{z}z\right\} 
+ \left(c_{1\sigma}b_{00}^{1\sigma} + c_{2\sigma}b_{00}^{2\sigma}\right) 
\times \exp\left\{-i\pi\frac{E_{2\sigma} - E_{1\sigma}}{E_{0}}k_{z}z\right\}\psi_{00}^{b}(\mathbf{R} - \mathbf{R}_{b}) 
\times \exp\left\{-i\pi\frac{E_{1\sigma}}{E_{0}}k_{z}z\right\}.$$
(24)

It can be shown that if the overlap between  $\psi^a_{00}(\mathbf{R}-\mathbf{R}_a)$ ,  $\psi^b_{00}(\mathbf{R}-\mathbf{R}_b)$ ,  $U^a(\mathbf{R}-\mathbf{R}_a)$  and  $U^b(\mathbf{R}-\mathbf{R}_b)$  is negligible,  $a^{1\sigma}_{00}$  and  $b^{2\sigma}_{00}$  tend to zero. The wavefunction can then be written as

$$\Psi(\mathbf{R}, z) \simeq 1 + c_{2\sigma} a_{00}^{2\sigma} \sin\left(\pi \frac{-E_{2\sigma}}{E_0} \frac{k_z}{2} z\right) \psi_{00}^a(\mathbf{R} - \mathbf{R}_a)$$

$$\times \exp\left\{-i\pi \left(\frac{E_{2\sigma}}{E_0} \frac{k_z}{2} z - \frac{1}{2}\right)\right\}$$

$$+ c_{1\sigma} b_{00}^{1\sigma} \sin\left(\pi \frac{-E_{1\sigma}}{E_0} \frac{k_z}{2} z\right) \psi_{00}^b(\mathbf{R} - \mathbf{R}_b)$$

$$\times \exp\left\{-i\pi \left(\frac{E_{1\sigma}}{E_0} \frac{k_z}{2} z - \frac{1}{2}\right)\right\}. \tag{25}$$

From this expression it is clear that the periodicity of excitation, as function of foil thickness, for different atom columns, can be different as is observed in experiments and simulations [18].

Note that, if the expansion of the  $\sigma_g$ ,  $\sigma_u$ ,  $1\sigma$  and  $2\sigma$  two-atom column system eigenfunctions is limited to the isolated atom column 1S eigenfunctions, localised at atom columns a and b, parameterised as quadratic two-dimensional normalised Gaussians or exponential function, the coefficients  $a_{00}^{1\sigma_g}$ ,  $b_{00}^{1\sigma_g}$ ,  $a_{00}^{1\sigma_u}$ ,  $b_{00}^{1\sigma_u}$ ,  $a_{00}^{1\sigma_u}$ ,  $b_{00}^{1\sigma_u}$ ,  $a_{00}^{1\sigma_u}$ ,  $a_{00}^{1\sigma_u}$ ,  $a_{00}^{2\sigma_u}$  and  $b_{00}^{2\sigma_u}$  as well as the eigenenergies  $E_{1\sigma_g}$ ,  $E_{1\sigma_u}$ ,  $E_{1\sigma}$  and  $E_{2\sigma}$  can be calculated analytically as is reported in Ref. [33] (Gaussian).

4.5. The S-state model for an assembly of atom columns

The reader will have noticed that Eqs. (3), (21) and (25) are closely related to each other. These expressions will be generalised as

$$\Psi(\mathbf{R}, z) \simeq 1 + 2 \sum_{j} c_{1}^{j} \sin\left(\pi \frac{-E_{1}^{j}}{E_{0}} \frac{k_{z}}{2} z\right) \psi_{1}^{j} (\mathbf{R} - \mathbf{R}_{j})$$

$$\times \exp\left\{-i\pi \left(\frac{E_{1}^{j}}{E_{0}} \frac{k_{z}}{2} z - \frac{1}{2}\right)\right\}, \tag{26}$$

where j labels the atom columns in the crystal. If it is assumed that the most bound local eigenfunction  $\psi_1^j(\mathbf{R} - \mathbf{R}_j)$  can be approximated well as a two-dimensional Gaussian or exponential function, both quadratic normalised, as shown in Section 3.

$$\psi_1^j(\mathbf{R} - \mathbf{R}_j) = \sqrt{\frac{|E_1^j|}{\pi}} \frac{1}{b_j} \exp\left(-\frac{1}{2} \left(\sqrt{|E_1^j|} \frac{(\mathbf{R} - \mathbf{R}_j)}{b_j}\right)^2\right), \quad (27)$$

or

$$\psi_1^j(\mathbf{R} - \mathbf{R}_j) = \sqrt{\frac{|E_1^j|}{2\pi}} \frac{1}{b_j} \exp\left(-\frac{1}{2} \left(\sqrt{|E_1^j|} \frac{(\mathbf{R} - \mathbf{R}_j)}{b_j}\right)\right), \quad (28)$$

the wavefunction can be expressed in closed analytical form. Henceforth it will be called the analytical S-state model. The wavefunction is now completely determined by the parameters  $c_1^J$ ,  $E_1^J$ ,  $b_i$ , z and  $\mathbf{R}_i$ . This allows a significant gain in calculation speed compared to iterative methods as Bloch wave- or multislice algorithms. At the other hand, is such an analytic model for the wavefunction, very well suited to invert the dynamical electron scattering. In order to do this, the parameters must be estimated by means of a parameter estimation technique. Since the model for the wavefunction is analytical, also the gradient of  $\Psi(\mathbf{R},z)$  and the Hessian matrix can be provided analytically, which allows fast convergence to the global optimum. The experimental data can be experimental reconstructed exit waves or  $C_s$ -corrected images.

4.6. Accuracy of the S-state model for an assembly of atom columns

The S-state model is only an approximate description of a dynamical scattering process of an electron in a specimen foil. In this section we will study the limits of the model and the accuracy of the atom positions that can be expected.

As mentioned before, it is the main goal of the channelling theory to invert the dynamical electron scattering, which is equivalent with determination of the atom column positions and their chemical composition. Here we will mainly focus on the positions of the atom columns  $\mathbf{R}_i$ . In order to evaluate the accuracy to which the atom columns positions can be determined, multislice simulations of exit waves of known test structures are performed and used as observations, to which an analytic S-state model was optimised using a criterion. Noise was not taken into account. The estimated atom column positions  $\mathbf{R}_i$  are then compared to the initial atom column positions used as input for the multislice calculations. From this, the accuracy or systematic error of the estimated atom column positions can be studied. Note that this test does not provide information about the statistical precision but only about the accuracy of the model.

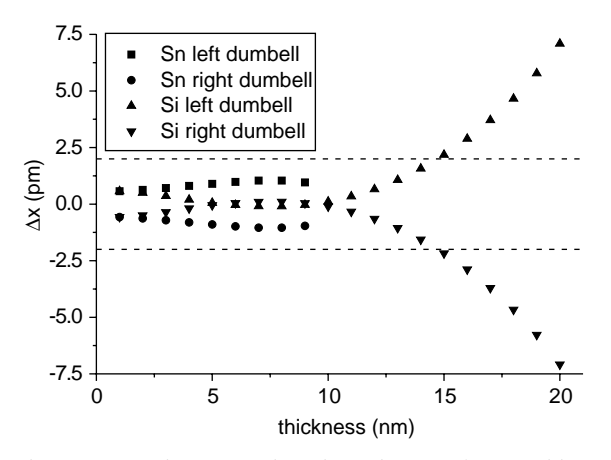


Fig. 6. Systematic error on the estimated atom column position of both the left and right atom column of a dumbbell, along [0 0 1], for both Si [1 1 0] and Sn [1 1 0]. The dotted line marks 2 pm.

As fitting criterion, "least squares" are used. As test structures Si [1 1 0], Sn [1 1 0] and GaN [1 1 0] are chosen, because of the small spacing between

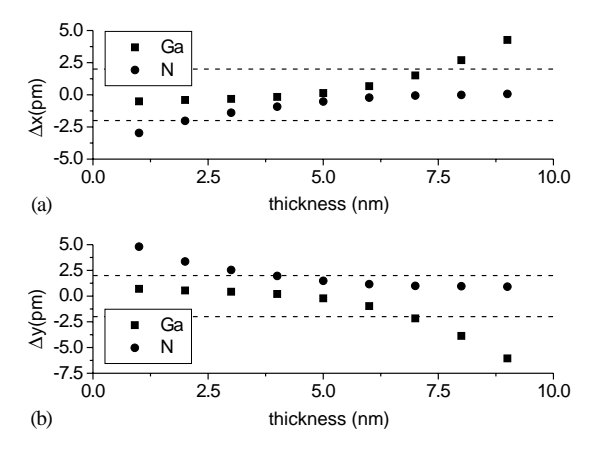


Fig. 7. Systematic error on the estimated atom column position of both Ga and N along the *x*-direction (a) and the *y*-direction (b). The dotted line marks 2 pm.

the atom columns in the [110] orientation, respectively, 136, 162 and 113 pm. All parameters mentioned in the previous section are fitted. From Fig. 6 it is clear that the accuracy of the estimated atom column positions is better than 10 pm for Si [110] and 1.5 pm for Sn [110] up to about 70–80% of  $D_{00}$ , the periodical thickness, which is about 30 nm for Si [1 1 0] and 10 nm for Sn [1 1 0]. Note that the accuracy on the atom column positions is better than 2 pm for both Si [1 1 0] and Sn [1 1 0] up to a thickness of 10 nm. Fig. 7 shows that the accuracy of the estimated atom column positions in the x- and y-direction is better 5 pm for both the Ga and N atom columns of GaN [1 1 0], up to a thickness of 9 nm about 80% of the periodical thickness  $D_{00} \simeq 11$  nm of the Ga atom columns. For small thicknesses the positions of the Ga atom columns can be estimated more accurately than the positions of the N atom columns, whereas thicknesses near the periodical thickness  $D_{00}$  of the Ga atom columns, the N atom

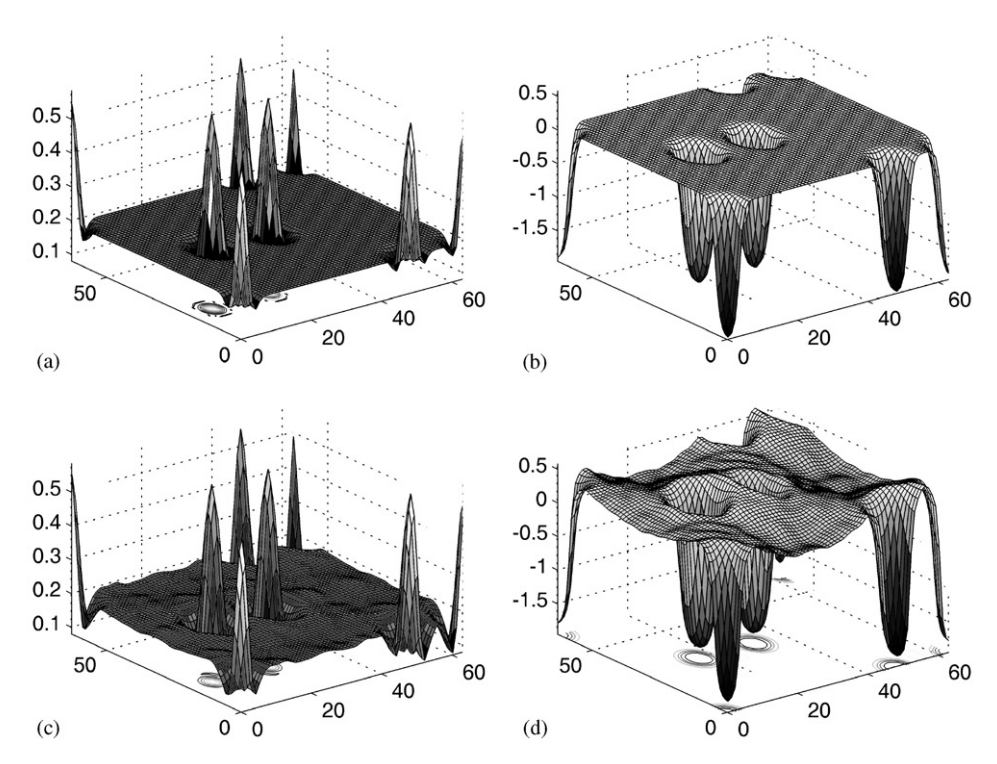


Fig. 8. Electron wave of Sn [1 1 0] at a specimen foil thickness of 9 nm: (a) amplitude of the fitted analytical S-state model; (b) the phase of the fitted analytical S-state model; (c) amplitude calculated with a multislice formalism; (d) the phase calculated with a multislice formalism.

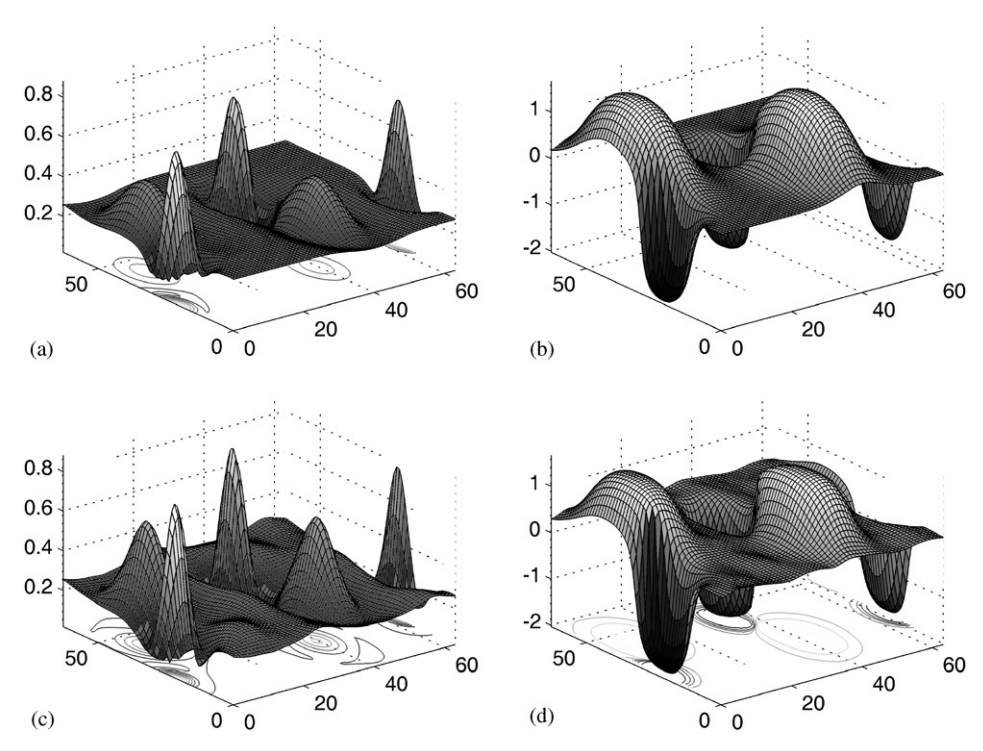


Fig. 9. Electron wavefunction of GaN [1 1 0] at a specimen foil thickness of 8 nm. (a) amplitude of the fitted analytic S-state model; (b) the phase of the fitted analytic S-state model; (c) amplitude calculated with a multislice formalism; (d) the phase calculated with a multislice formalism.

column positions can be estimated more accurately than the Ga atom column positions. Figs. 8 and 9 show the amplitude and phase of respectively the fitted analytic S-state model and the wavefunction calculated with a multislice algorithm, for Sn [1 1 0] (z=9 nm) and GaN [1 1 0] (z=8 nm). From this it can be concluded that the S-state model provides a quite robust model to estimate the atom column positions with high accuracy, from an electron wavefunction of crystals even with closely spaced atom columns.

# 5. Electron channelling theory in case of tilted illumination

In practice it is almost impossible to align the specimen locally in zone-axis orientation. This is due, for example, to local bending of the specimen or different grain orientations. Therefore, it is

important for practical applicability of the channelling theory, that the effect of crystal- and beam tilt is included in the model and can be estimated. Tilt was included in the channelling theory by Van Dyck et al. [34] in a different and more complicated way, nevertheless the conclusions are similar.

Both crystal- and beam tilt can be regarded as equivalent if the description is restricted to the interaction between electron and specimen. Since the treatment of beam tilt is more straightforward than the treatment of crystal tilt, beam tilt will be considered here. In these cases  $k_R$ , the two-dimensional radial component, parallel to the surface of the specimen foil, of the wavevector k of the incident plane wave, is nonthree-dimensional time-independent Schrödinger equation of an electron in a "forward two-dimensional potential, in the scattering approximation", can be written as follows:

$$-\frac{2\pi\hbar^{2}k_{z}}{\mu i}\frac{\partial}{\partial z}\Psi(\mathbf{R},z)e^{2\pi i\mathbf{k}_{\mathbf{R}}\cdot\mathbf{R}}$$

$$=H\Psi(\mathbf{R},z)e^{2\pi i\mathbf{k}_{\mathbf{R}}\cdot\mathbf{R}}-\frac{4\pi^{2}\hbar^{2}k_{R}^{2}}{2\mu}\Psi(\mathbf{R},z)e^{2\pi i\mathbf{k}_{\mathbf{R}}\cdot\mathbf{R}}.$$
(29)

Since H is not dependent on z, the wavefunction  $\Psi(\mathbf{R},z)$  can be written as a series of solutions, similar as Eq. (1), factorised in **R**-dependent eigenfunctions  $\psi_{nm}(\mathbf{R})$  and z-dependent phase factors

$$\Psi(\mathbf{R}, z)e^{2\pi i \mathbf{k}_{\mathbf{R}} \cdot \mathbf{R}} = \sum_{nm} c_{nm}(\mathbf{k}_{\mathbf{R}}) \psi_{nm}(\mathbf{R})$$

$$\times \exp\left\{-i\pi \left(\frac{E_{nm}}{E_0} - \frac{k_R^2}{k_z^2}\right) k_z z\right\}.$$
(30)

Note that  $c_{nm}(\mathbf{k_R})$  is now dependent on  $\mathbf{k_R}$ . This equation can be rewritten, using the boundary condition  $\sum_{nm} c_{nm}(\mathbf{k_R}) \psi_{nm}(\mathbf{R}) = \Psi(\mathbf{R}, 0) e^{2\pi i \mathbf{k_R} \cdot \mathbf{R}} = e^{2\pi i \mathbf{k_R} \cdot \mathbf{R}}$ .

$$\Psi(\mathbf{R}, z) = 1 + \sum_{nm} 2c_{nm}(\mathbf{k_R})$$

$$\times \sin\left(-\pi \left(\frac{E_{nm}}{E_0} - \frac{k_R^2}{k_z^2}\right) \frac{k_z}{2} z\right) \psi_{nm}(\mathbf{R})$$

$$\times \exp\left\{-i\pi \left(\left(\frac{E_{nm}}{E_0} - \frac{k_R^2}{k_z^2}\right) \frac{k_z}{2} z\right) + 2\mathbf{k_R} \cdot \mathbf{R} - \frac{1}{2}\right)\right\}.$$
(31)

After substitution of Eq. (30) or Eq. (31) in Eq. (29) it is clear that the differential equation can be transformed to the known eigenvalue problem equation (2), in case of plane wave illumination along a main zone-axis.

Eq. (31) is not an exact description of the wavefunction up to high tilt angles. The breakdown will happen if the approximations made in Eq. (29) are not justified anymore. For large beam tilts, the backscattering cannot be neglected and thus the "forward scattering approximation" is no longer valid. However, for realistic tilt angles, as occurring in HRTEM, the S-state model is valid as will be shown in the next section.

The periodical thickness  $D_{nm}^{\mathbf{k_R}}$  of the eigenfunctions  $\psi_{nm}(\mathbf{R}, z)$  is not invariant under tilt  $\mathbf{k_R}$  and is

equal to

$$D_{nm}^{\mathbf{k_R}} = \frac{2}{k_z} \frac{1}{(k_R^2/k_z^2) - E_{nm}/E_0}$$
$$= D_{nm}^0 \sqrt{1 + \tan^2 \alpha} \left( 1 + \frac{D_{nm}^0}{2\lambda} \tan^2 \alpha \right)^{-1}. \quad (32)$$

since  $|\mathbf{k_R}|/|\mathbf{k_z}| = \tan \alpha$  and  $k_z = (1/\lambda)(1/\sqrt{1 + \tan^2 \alpha})$  with  $\alpha$  the tilt angle. If  $\alpha$  is small,  $D_{nm}^{\mathbf{k_R}}$  can be written to a good approximation as

$$D_{nm}^{\mathbf{k_R}} \simeq D_{nm}^0 \left( 1 + \frac{D_{nm}^0}{2\lambda} \alpha^2 \right)^{-1}.$$
 (33)

The periodical thickness will thus decrease as function of increasing tilt, as if the electron-object interaction increases. This is seems surprising, since it is expected that the strength of the electron-object interaction decreases in case of increasing tilt. However this is only part of the story. In the next we will show that indeed the electron-object interaction decreases as expected.

The eigenfunctions  $\psi_{nm}(\mathbf{R})$  can be classified in three groups. A first group is the 1S eigenfunction  $\psi_{00}(\mathbf{R})$ , which has an absolute eigenenergy which is much larger than zero. A second group comprises the less bound eigenfunctions, which have a much smaller absolute eigenenergy as the 1S eigenfunction. Some of these eigenfunction were not excited, in case of plane wave illumination along a main zone-axis, due to their symmetry. A third group comprises the continuum eigenfunctions, which have an eigenenergy which is approximately equal to  $E_t = h^2 k_R^2 / 2m \simeq (k_R^2 / k_z^2) E_0$ , the transverse energy of the incident electrons. It can be shown that only these continuum eigenfunctions are excited since they are close to the plane wave  $e^{2\pi i \mathbf{k_R} \cdot \mathbf{R}}$ outside the atom column.

If we now consider for example a Si [1 0 0] atom column, which has only one bound eigenfunction, the 1S eigenfunction, there are only eigenfunctions of group one and three involved. We can now to a good approximation expand, the terms containing eigenfunctions of the third group of Eq. (31) up to first order in  $-\pi(E_{nm\in C}/E_0 - k_R^2/k_z^2)(k_z/2)z$ , since  $E_{nm\in C} \simeq (k_R^2/k_z^2)E_0$ . "C" is labeling the continuum eigenfunctions.

$$\Psi(\mathbf{R}, z) \simeq 1 + 2c_{00}(\mathbf{k_R})$$

$$\times \sin\left(-\pi \left(\frac{E_{00}}{E_0} - \frac{k_R^2}{k_z^2}\right) \frac{k_z}{2} z\right) \psi_{00}(\mathbf{R})$$

$$\times \exp\left\{-i\pi \left(\left(\frac{E_{00}}{E_0} - \frac{k_R^2}{k_z^2}\right) \frac{k_z}{2} z\right) + 2\mathbf{k_R} \cdot \mathbf{R} - \frac{1}{2}\right)\right\}$$

$$+ \sum_{nm \in C} 2ic_{nm}(\mathbf{k_R}) \left(-\pi \left(\frac{E_{nm}}{E_0} - \frac{k_R^2}{k_z^2}\right) \frac{k_z}{2} z\right)$$

$$\times \psi_{nm}(\mathbf{R}) e^{-2\pi i \mathbf{k_R} \cdot \mathbf{R}}.$$
(34)

It can be easily shown that the excitation coefficient  $c_{00}(\mathbf{k_R}) = \int \psi_{00}^*(\mathbf{R}) \mathrm{e}^{2\pi \mathrm{i} \mathbf{k_R} \cdot \mathbf{R}} \, \mathrm{d}\mathbf{R}$  is decreasing with increasing tilt. The second term of Eq. (34) is thus gaining in importance compared to the first term, containing the 1S eigenfunction. The thickness dependence of the wavefunction thus becomes much more linear as a function of thickness. Physically this means that fewer electrons are trapped in the atom column and that the electron–object interaction is closer to a kinematic model than it is in the non-tilted case. Tilt thus breaks down the strong dynamical interaction as is expected.

For a heavier atom column, like a Au [100] atom column, eigenfunctions of the second group are contributing as well to Eq. (34). Although  $E_{nm} - (k_R^2/k_z^2)E_0$  are small, an expansion up to first order in  $-\pi(E_{nm}/E_0 - k_R^2/k_z^2)(k_z/2)z$  would be insufficient. This group of eigenfunctions will thus introduce non-linear terms as a function of thickness in Eq. (34), apart from the term with the 1S eigenfunction. Nevertheless the excitation coefficients  $c_{nm\notin C}(\mathbf{k_R})$  will decrease with increasing beam tilt, as will be shown in the next section. This confirms what we would expect, namely that for heavier atom columns a larger beam tilt is needed to reduce the dynamical interaction.

### 5.1. Excitation of the eigenfunctions

In case of plane wave illumination along a main zone-axis the eigenfunctions, which were not invariant under  $m_h$  and  $\mathscr{I}$ , were not excited e.g.  $\psi_{11x}(\mathbf{R})$  in case of an isolated atom column and  $\psi_{1\pi}(\mathbf{R})$  in case of an identical two-atom column

system. Nevertheless in case of tilted illumination, will the excitation coefficients of these eigenfunctions be different from zero depending on the direction of tilt. In order to evaluate the influence of tilt on the excitation of the eigenfunctions, the symmetry of the eigenfunctions multiplied by  $e^{2\pi i \mathbf{k_R} \cdot \mathbf{R}}$  will be studied. We first consider the behaviour of the real and imaginary part of  $e^{2\pi i \mathbf{k_R} \cdot \mathbf{R}}$  when acted on by operations  $m_h$  and  $\mathscr{I}$ 

$$m_{\rm h} \cos(2\pi \mathbf{k_R} \cdot \mathbf{R}) = (\cos(2\pi k_x x) \cos(2\pi k_y y) + \sin(2\pi k_x x) \sin(2\pi k_y y)),$$

$$m_{\rm h} \sin(2\pi \mathbf{k_R} \cdot \mathbf{R}) = (\sin(2\pi k_x x)\cos(2\pi k_y y) - \cos(2\pi k_x x)\sin(2\pi k_y y))$$
(35)

and

$$\mathcal{I}\cos(2\pi\mathbf{k}_{\mathbf{R}}\cdot\mathbf{R}) = \cos(2\pi\mathbf{k}_{\mathbf{R}}\cdot\mathbf{R}),$$

$$\mathcal{I}\sin(2\pi\mathbf{k}_{\mathbf{R}}\cdot\mathbf{R}) = -\sin(2\pi\mathbf{k}_{\mathbf{R}}\cdot\mathbf{R}).$$
(36)

It can be concluded that neither the real nor the imaginary part is invariant under mirror-axis  $m_h$ , at least not, if both  $k_x$  and  $k_y$  are different from zero. The real part is invariant under inversion  $\mathcal{I}$ , whereas the imaginary part is not invariant.

Combining both the behaviour of the eigenfunctions and  $e^{2\pi i k_{\mathbf{R}} \cdot \mathbf{R}}$  when acted on by operation  $\mathscr{I}$ , using  $\mathscr{I}(g(\mathbf{R})h(\mathbf{R})) = \mathscr{I}(g(\mathbf{R}))\mathscr{I}(h(\mathbf{R}))$ , it can be concluded that the excitation of the eigenfunctions which are invariant under inversion  $\mathscr{I}$ , will be real and that the ones which are not invariant under inversion  $\mathscr{I}$ , will be imaginary. Since all excitation coefficients are either real or imaginary, their phases are 0 and  $\pi/2$  or  $-\pi/2$ , respectively.

In case of an isolated atom column, the excitation coefficient of  $\psi_{n0}(\mathbf{R})$  will be real and, for example, the excitation coefficients of  $\psi_{11_x}(\mathbf{R})$  and  $\psi_{11_y}(\mathbf{R})$  will be imaginary. In case of a two-atom column system the excitation coefficients of  $\psi_{\sigma_g}(\mathbf{R})$  and  $\psi_{\pi_g}(\mathbf{R})$  will be real and the excitation coefficients of  $\psi_{\sigma_u}(\mathbf{R})$  and  $\psi_{\pi_u}(\mathbf{R})$  will be imaginary. If  $k_x = 0$ ,  $\psi_{11_x}(\mathbf{R})$ ,  $\psi_{\sigma_u}(\mathbf{R})$  and  $\psi_{\pi_g}(\mathbf{R})$  are not excited and if  $k_y = 0$ ,  $\psi_{11_y}(\mathbf{R})$  and  $\psi_{\pi}(\mathbf{R})$  are not excited. This could be concluded from the behaviour of the eigenfunction multiplied by  $e^{2\pi i \mathbf{k}_{\mathbf{R}} \cdot \mathbf{R}}$  when acted on by operation  $m_h$ , using  $m_h(g(\mathbf{R})) h(\mathbf{R})$ ) =  $m_h(g(\mathbf{R}))m_h(h(\mathbf{R}))$ .

In Fig. 10,  $|c_p(\mathbf{k_R})\sin(-\pi(E_p/E_0 - k_R^2/k_z^2))|$  for different two-atom column system

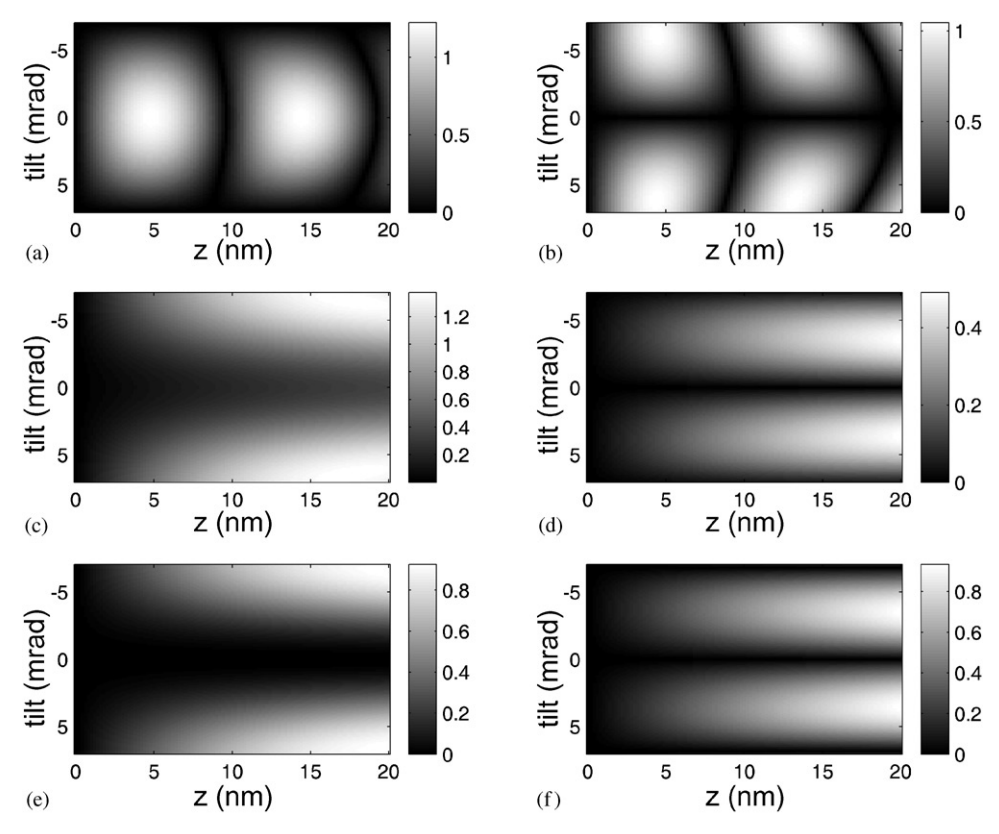


Fig. 10.  $|c_p(\mathbf{k_R})\sin(-\pi(E_p/E_0 - k_R^2/k_z^2)(k_z/2)z)|$  as a function of specimen foil thickness z and tilt  $\mathbf{k_R}$ , respectively, for  $1\sigma_g$  (a),  $1\sigma_u$  (b),  $2\sigma_g$  (c),  $1\pi_u$  (d),  $1\pi_g$  (e) and  $2\sigma_u$  (f). The excitations and eigenergies were calculated for a dumbbell of Sn [1 1 0].

eigenfunctions, of a dumbbell of Sn [1 1 0], are plotted as a function of thickness and crystal tilt, for the case that both  $k_x \neq 0$  and  $k_y \neq 0$ . It is clear that for tilts larger than a few mrad, for a dumbbell of Sn [1 1 0], the S-state model is no longer valid, since the wavefunction is no longer governed by the  $1\sigma_g$ - or the 1S eigenfunction.

### 5.2. An additional effect of tilted illumination

Tilted illumination will introduce different kinds of effects, which will alter the wavefunction. Most of them were discussed in detail in the previous paragraphs, like the decrease of the periodical thickness and the excitation of eigenfunctions with  $\pi$  or "ungerade" like symmetry due to the nonsymmetrical illumination.

One effect which was not discussed in the previous sections is the extra factor  $e^{2\pi i \mathbf{k_R} \cdot \mathbf{R}}$ , which will cause a shift of the maxima and minima of the amplitude and phase of the wavefunction with respect to non-tilted illumination. In a fitting procedure this will lead to biased estimations of the atom column positions. This can be avoided by including two extra parameters  $(k_x, k_y)$ , which can be position dependent if the crystal foil is for example locally bended.

### 6. Guidelines for experimentalists

In this section the authors would like to draw some clear conclusions to guide experimentalists. In our opinion, the channelling theory has a large potential, not just as teaching and understanding tool, but also as a model, which allows to invert the dynamic scattering to a good approximation. It is actually in this framework that we like to discuss the limits of the channelling theory in this section, more specific the effect on the estimated atom column positions by neighbouring atom columns and beam- or crystal tilt. Although it is difficult to give some hard numbers we will try to give an idea about the limits.

First of all we like to stress that the S-state model is only an approximate description of a dynamical scattering process. For example only the 1S eigenfunction is kept, whereas the other eigenfunctions are neglected. This approximation is only valid up to a thickness of about 80% of the periodical thickness  $D_{00} = -(2/k_z)(E_0/E_{00})$ .  $D_{00}$  is dependent on the kinetic energy of the incident electrons  $E_0$  and the eigenenergy of the 1S eigenfunction of the atom column  $E_{00}$ .  $E_{00}$  can be roughly estimated by Eq. (4) and the parameter  $\beta$  provided by Van Dyck et al. [27].  $D_{00}$  is for most atom column types of the order of the upper limit of the range of specimen thicknesses, normally used for high-resolution electron microscopy.

Second, the S-state model assumes that the wavefunction of the columnar structure is equal to the superposition of the wavefunctions of the constituting atom columns. This is in principle only the case if the atom columns can be regarded as isolated. Nevertheless, if the atom column positions are symmetry positions of the structure, the estimated atom column positions will not be influenced by it, since the minima and maxima of the wavefunction are not moved. Even if the atom columns positions are no symmetry positions of the structure, it was shown in Section 4 that the effect of neighbouring atom columns, on systems with  $2m_h m_v$  or  $m_h$  symmetry, on the estimated atom column positions is smaller than 5 pm for thicknesses up to 10 nm, for closely spaced atom columns like the dumbbells in Si [1 1 0], Sn [1 1 0] and GaN [1 1 0], with respectively an atom column spacing of 136, 162, 113 pm. For simplicity, we have considered a two-atom column system, however the results can be generalised for general assemblies of atom columns.

Third, the S-state model assumes plane wave illumination along a main zone-axis. In Section 5 it

is shown that the model can easily be extended for the case of tilted illumination or equivalent crystal tilt. It is shown that the amount of tilt is limited, since for large tilts the weakly bound non-S eigenfunctions will be excited as well. Nevertheless this will only be significant for tilts larger than a few mrad. The S-state model is thus still valid, even in case of a small tilt of a few mrad. Nevertheless it would be worthwhile to include extra fitting parameters  $(k_x, k_y)$ , since the extra factor  $e^{2\pi i \mathbf{k_R} \cdot \mathbf{R}}$  in the wavefunction can introduce some shift of the minima and maxima of the amplitude and phase of the wavefunction.

As a general conclusion we can state that the Sstate model is valid up to thicknesses normally used in high-resolution electron microscopy, and that even for closely spaced atoms and slightly tilted illumination. Because of its simplicity and the possibility to express it in a closed analytical form, the method has the potential to become a real work horse for HRTEM. It allows to interpret the reconstructed electron wavefunction directly in terms of the projected structure, yielding an approximate structure model that can then further be used as a starter for quantitative refinement. Furthermore it is valid even for crystal defects (dislocations, translation interfaces, etc.) as long as the atoms are aligned in columns close to the beam direction.

### Acknowledgements

The first author gratefully acknowledges the support of the institute for the promotion of innovation by science and technology in Flanders (IWT).

# Appendix A. Calculation of the bound eigenfunctions of an isolated atom column

In this section an isolated atom column will be considered. The system poses rotational symmetry, that is all directions in the plane are equivalent. The potential of such a system will only depend on the radial distance  $\rho$  from a suitably chosen origin, this means  $U(\mathbf{R}) = U(\rho)$  with  $\rho = |\mathbf{R}|$ . Such a

problem is known in physics as a central force problem. In this case, the solution of Eq. (2) may be factorised as

$$\psi_{nm}(\mathbf{R}) = R_{nm}(\rho)\Phi_m(\varphi) \tag{A.1}$$

with  $\Phi_m(\varphi)$  the angular function and  $R_{nm}(\rho)$  the radial function, which are solutions of

$$\frac{\partial^2}{\partial \varphi^2} \Phi_m(\varphi) = -m^2 \Phi_m(\varphi) \tag{A.2}$$

and

$$-\left\{\frac{\hbar^2}{2\mu}\left(\frac{\partial^2}{\partial\rho^2} + \frac{1}{\rho}\frac{\partial}{\partial\rho} - \frac{m^2}{\rho^2}\right) + eU(\rho)\right\}R_{nm}(\rho)$$

$$= E_{nm}R_{nm}(\rho) \tag{A.3}$$

respectively. In the following sections, the solutions of these equations will be discussed.

### A.1. Solutions of the angular equation

Eq. (A.2) is known from the elementary theory of ordinary differential equations. Two elementary independent solutions are  $e^{im\varphi}$  and  $e^{-im\varphi}$ . Therefore,  $\Phi_m(\varphi)$  can be written as

$$\Phi_m(\varphi) = \frac{1}{\sqrt{2\pi}} e^{im\varphi}.$$
 (A.4)

If m is an integer  $(m=0,\pm 1,\pm 2,...)$  this set of functions is orthonormal. Standing wave representations of  $\Phi_m(\varphi)$  can be formed by defining appropriate linear combinations. For example for  $m=\pm 1$ 

$$\Phi_{1_x}(\varphi) = \frac{1}{\sqrt{\pi}} \cos \varphi, 
\Phi_{1_y}(\varphi) = \frac{1}{\sqrt{\pi}} \sin \varphi.$$
(A.5)

### A.2. Solutions of the radial equation

The solution of the radial equation (A.3) is much more difficult to solve than the angular equation. In the past various attempts were made to solve it numerically. These attempts can be mainly categorised in two groups: finite difference methods [15,35] and expansion of the eigenfunc-

tions in a set of basis functions [15]. Both methods have their particular advantages and disadvantages, which will be discussed below.

If one tries to solve Eq. (A.3) by finite difference methods one is faced with divergence problems in the origin of the term

$$\frac{1}{\rho} \frac{\partial}{\partial \rho} - \frac{m^2}{\rho^2}.$$
 (A.6)

This divergence can be avoided for m=0. However this puts restrictions on the eigenfunctions that can be calculated by this method. In Ref. [15], two other numerical problems are reported. The first problem is that the radial range has to be restricted to [0, L] in order to limit the number of sampling points, and thus the order of the eigenmatrix. This implies that only these bound functions, which are sufficiently damped, can be calculated correctly. The second problem is that the equation is not defined for negative values so that asymmetric difference formula has to be used to approximate the derivatives in the neighbourhood of the boundaries. Their use will destroy the symmetry of the eigenmatrix and so the hermicity and consequently the eigensolutions of the matrix will not necessarily form a complete basis. The last mentioned problem is tackled if the Laplacian term is written in cartesian coordinates. Note that it is then easy to incorporate two-atom column potentials and calculate the eigenfunctions of two neighbouring atom columns.

Expansion of the eigenfunctions in an orthonormal and complete basis will avoid large sampling in order to correctly describe the sharp peak of the potential. When an optimal basis is chosen, the number of basis functions needed is limited. This reduces the dimension of the eigenvalue problem which has to be solved. In the past Bessel functions were proposed as basis set, which are orthonormalised on an interval [0, L] [15]. The advantage is that the elements of the eigenmatrix can be calculated analytically if one is making use of the Doyle and Turner parameterisation [23], to describe the two-dimensional mean atom column potential. A disadvantage is that an interval [0, L]has to be chosen on which the basis is orthonormal. The larger the interval the larger the number of basis functions which has to be taken into account to achieve convergence. Although the number of basis functions needed to describe the 1S eigenfunction is limited, Bessel functions are not an optimal basis set to expand in. A much more effective basis set are two-dimensional quantum harmonic oscillator eigenfunctions which are orthonormal and complete over the whole space. Only a limited number of basis functions is needed, if the harmonic oscillator length is optimised to the studied problem. To describe the most bound eigenfunction, only one is to good approximation sufficient, which will be argued in the next section. The elements of the eigenmatrix can not be calculated analytically but a recursion relation can be set up if one is making use of the Doyle and Turner parameterisation. A detailed description of this will be beyond the goal of this paper and will be reported elsewhere.

# Appendix B. A fast method to calculate $E_{00}$ and the 1S-eigenfunction

It could be concluded from Section 3 that the most bound eigenfunction of an atom column can be reasonably described as a two-dimensional quadratic normalised Gaussian or exponential function. This deduction was drawn based on calculations of the most bound eigenfunction, by finite difference and expansion in a set of basis functions, of an atom column and from physical intuition. Two parameters are unknown in this parameterisation of the  $\psi_{00}(\rho)$  eigenfunction; b and  $E_{00}$ . In order to improve a guess for b and  $E_{00}$ the variational principle will be used [36]. This method will provide the possibility to calculate  $E_{00}$ in an easy and quite accurate way compared to a solution obtained by finite difference methods and an expansion in a basis set as sketched in Appendix A.

Assume that the Gaussian parameterisation of the 1S eigenfunction of the atom column is written as

$$\psi_{00}(\rho, b') = \frac{1}{\sqrt{\pi b'}} \exp\left(-\frac{1}{2} \left(\frac{\rho}{b'}\right)^2\right),\tag{B.1}$$

with  $b' = b/\sqrt{|E_{00}|}$  variable. Then the variational principles states that

$$E_{00} \leqslant H(b') = \frac{\int \psi_{00}(\rho, b') H \psi_{00}(\rho, b') \rho \, d\rho}{\int \psi_{00}(\rho, b') \psi_{00}(\rho, b') \rho \, d\rho}.$$
 (B.2)

In order to minimise H(b') the integrals in Eq. (B.2) has to be solved. The Doyle and Turner [23] parameterisation is used to describe the two-dimensional mean atom column potential  $U(\rho)$ .

$$U(\rho) = \frac{\hbar^2}{2\mu e} \sum_{i} \frac{A_i}{B_i} \exp\left(-\frac{\rho^2}{B_i}\right)$$
 (B.3)

with

$$A_i = \frac{4\mu/\mu_0}{d}a_i$$
 and  $B_i = \frac{b_i + B}{4\pi^2}$ , (B.4)

with  $a_i$  and  $b_i$  the Doyle and Turner parameters and  $\mu_0$  the relativistic rest mass of an electron. Note that this expression for the mean atom column potential is an expression for the case that all atoms in the atom column are equal. Of course this expression can be extended to one for different kind of atom types in one atom column. The nominator of Eq. (B.2) is one since the eigenfunctions are normalised, H(b') can then be written as

$$H(b') = \frac{E_0}{k^2} \left( \frac{1}{b'^2} - \sum_i \frac{A_i}{B_i + b'^2} \right).$$
 (B.5)

In order to estimate  $E_{00}$ , H(b') has to be minimised by solving the equation

$$\left. \frac{\partial H(b')}{\partial b'} \right|_{b'=b'_{\min}} = 0$$

or

$$\sum_{i} \frac{A_{i}}{(B_{i} + b_{\min}^{\prime 2})^{2}} = \frac{1}{b_{\min}^{\prime 4}},$$
(B.6)

which results in

$$E_{00} \simeq \frac{E_0}{k^2} \left( \frac{1}{b_{\min}^{'2}} - \sum_i \frac{A_i}{B_i + b_{\min}^{'2}} \right)$$

$$\simeq \frac{E_0}{k^2} \left( \frac{1}{b_{\min}^{'2}} - \sum_i \frac{4(\mu/\mu_0)a_i}{d((b_i + B)/4\pi^2 + b_{\min}^{'2})} \right).$$
(B.7)

Similarly as for a Gaussian H(b') can be calculated assuming that the 1S eigenfunction of the atom

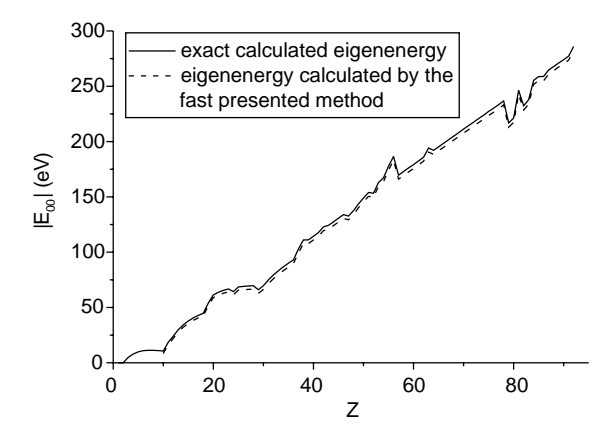


Fig. 11. Absolute value of the eigenenergy  $E_{00}$  calculated by expansion of the eigenfunctions in a basis of two-dimensional harmonic oscillators and by the fast presented method (Gaussian parameterisation), using the variational principle. The repeat distance d is assumed to be 0.4 nm.

Table 1 (a) Repeat distance in the atom column. (b and c) Eigenenergy  $E_{00}$  calculated by expansion of the eigenfunctions on the basis of two-dimensional harmonic oscillator eigenfunctions (b) and by the presented fast method (Gaussian parameterisation), using the variational principle (c).

Z	(a) d (nm)	(b) E <sub>00</sub> (eV)	(c) E <sub>00</sub> (eV)
Si	0.5431	-20.11	-18.42
Cu	0.3615	-78.12	-74.95
Sr	0.608	-57.11	-54.30
Sn	0.6489	-69.61	-66.63
Au	0.40786	-210.27	-206.82

column can be parameterised by an exponential function

$$\psi_{00}(\rho, b') = \frac{1}{\sqrt{2\pi}b'} \exp\left(-\frac{1}{2}\left(\frac{\rho}{b'}\right)\right). \tag{B.8}$$

H(b') can then be written as

$$H(b') = \frac{E_0}{k^2} \left[ \frac{1}{b^{2'}} - 2 \sum_{i} \frac{A_i}{b^{2'}} \left( 1 - \sqrt{\pi} \frac{\sqrt{B_i}}{b'} \exp\left(\frac{B_i}{b^2}\right) \right) \times \left( 1 - \operatorname{Erf}\left(\frac{\sqrt{B_i}}{b'}\right) \right) \right].$$
 (B.9)

After minimisation of this equation as function of b',  $E_{00}$  can be estimated. Our experience is that for small values of the Debye–Waller factor, the

parameterisation of the 1S eigenfunction as an exponential function provides better estimates of  $E_{00}$  than a Gaussian parameterisation. Although, in practice it is much more simple to minimise Eq. (B.5) than Eq. (B.9), the latter is in some particular situations unstable.

The variational principle provides thus a very effective and quite accurate method to calculate the eigenenergy of an atom column. In Fig. 11 both the eigenenergies, calculated with the presented method (using a Gaussian parameterisation) and by means of expansion in a basis set for constant d and B, for various atom types Z are plotted. In Table 1 some hard numbers of the eigenenergy of particular well-known isolated atom columns are given, calculated by expansion of the eigenfunctions on the basis of two-dimensional harmonic oscillator eigenfunctions and by the presented fast method (Gaussian parameterisation), using the variational principle. As is clear from Fig. 11 and Table 1 the match is quite good.

#### References

- [1] E.J. Kirkland, Ultramicroscopy 15 (3) (1984) 151-172.
- [2] W.O. Saxton, J. Microsc. Spectrosc. Electron. 5 (5) (1980) 665–674.
- [3] H. Lichte, Ultramicroscopy 20 (3) (1986) 293-304.
- [4] W. Coene, G. Janssen, M. Op de Beeck, D. Van Dyck, Phys. Rev. Lett. 69 (26) (1992) 3743–3746.
- [5] W. Coene, A. Thust, M. Op de Beeck, D. Van Dyck, Ultramicroscopy 64 (1-4) (1996) 109–135.
- [6] H. Rose, Optik 85 (1) (1990) 19-24.
- [7] C.L. Jia, A. Thust, Phys. Rev. Lett. 82 (25) (1999) 5052–5055.
- [8] P. Geuens, O.I. Lebedev, G. Van Tendeloo, Solid State Commun. 116 (12) (2000) 643–648.
- [9] C. Kisielowski, C.J.D. Hetherington, Y.C. Wang, R. Kilaas, M.A. O'Keefe, A. Thust, Ultramicroscopy 89 (4) (2001) 243–263.
- [10] M. Haider, H. Rose, S. Uhlemann, E. Schwan, B. Kabius, K. Urban, Ultramicroscopy 75 (1) (1998) 53–60.
- [11] K. Urban, B. Kabius, M. Haider, H. Rose, J. Electron Microsc. 48 (6) (1999) 821–826.
- [12] A. Howie, Philos. Mag. 14 (1966) 223-237.
- [13] D. Van Dyck, J. Danckaert, W. Coene, E. Selderslaghs, D. Broddin, J. Van Landuyt, S. Amelinckx, The atom column approximation in dynamical electron-diffraction calculations, in: Computer Simulations of Electron Microscope Diffraction and Images, The Minerals, Metals and Materials Society, Warrendale, PA, 1989, pp. 107–134.

- [14] S.J. Pennycook, D.E. Jesson, Ultramicroscopy 37 (1–4) (1991) 14–38.
- [15] M. Op de Beeck, D. Van Dyck, Phys. Status Solidi A 150 (2) (1995) 587–602.
- [16] M. Op de Beeck, D. Van Dyck, Ultramicroscopy 64 (1–4) (1996) 153–165.
- [17] P.D. Nellist, S.J. Pennycook, Ultramicroscopy 78 (1–4) (1999) 111–124.
- [18] W. Sinkler, L.D. Marks, J. Microsc. (Oxford) 194 (1999) 112–123.
- [19] J. Lindhard, Mat.-Fys. Meddelelser Danske Videnskab Selskab 34 (14) (1965) 1.
- [20] A. Tamura, Y.H. Ohtsuki, Phys. Status Solidi B 62 (2) (1974) 477–480.
- [21] F. Fujimoto, Phys. Status Solidi A 45 (1) (1978) 99-106.
- [22] B.F. Buxton, J.E. Loveluck, J.W. Steeds, Philos. Mag. A 38 (3) (1978) 259–278.
- [23] P. Doyle, P. Turner, Acta Crystallogr. A 24 (1968) 390–397.
- [24] H. Yoshioka, J. Phys. Soc. Jpn. 12 (1957) 618.
- [25] C. Humphries, P. Hirsch, Philos. Mag. 18 (1968) 115.
- [26] D. Van Dyck, J. Chen, Acta Crystallogr. A 55 (1) (1999) 212–215.

- [27] D. Van Dyck, J. Chen, Solid State Commun. 109 (8) (1999) 501–505.
- [28] P. Geuens, J.H. Chen, A.J. den Dekker, D. Van Dyck, Acta Crystallogr. A 55 (Suppl. P11.OE.002.) (1999).
- [29] A. Tamura, T. Kawamura, Phys. Status Solidi B 73 (2) (1976) 391–400.
- [30] K. Komaki, F. Fujimoto, Phys. Lett. A 49 (6) (1974) 445–446.
- [31] F. Fujimoto, S. Takagi, K. Komaki, H. Koike, Y. Uchida, Radiat. Effects 12 (1972) 153–161.
- [32] M. Morisson, T. Estle, N. Lane, Quantum States of Atoms, Molecules and Solids, Prentice-Hall, Englewood Cliffs, NJ, 1976.
- [33] S. Van Aert, Quantitative high-resolution electron microscopy: channelling theory and its application on GaN, Masters, University of Antwerp, 1999.
- [34] D. Van Dyck, R.M.J. Bokel, H.W. Zandbergen, Microsc. Microanal. 4 (4) (1998) 428–434.
- [35] W. Sinkler, L.D. Marks, Ultramicroscopy 75 (4) (1999) 251–268.
- [36] J.J. Sakurai, Modern Quantum Mechanics, Revised Edition, Addison-Wesley, Reading, MA, 1994.